ELSEVIER

Journal of Chromatography A, 969 (2002) 301–311

JOURNAL OF CHROMATOGRAPHY A

www.elsevier.com/locate/chroma

Inverse gas chromatography study on partially esterified paper fiber

Peter Jandura[a], Bernard Riedl[b,*], Bohuslav Vaclav Kokta[a]

[a]*Centre de Recherches en Pâtes et Papiers, Université du Québec, C.P. 500, Trois-Rivières, Quebec, Canada G9A 5H7*
[b]*Département des Sciences du Bois, Faculté de Foresterie et de Géomatique/CERSIM, Université Laval, Pavillon Abitibi-Price, Quebec, Canada G1K 7P4*

Abstract

Paper fiber was treated in a heterogeneous esterification reaction with four different fatty acids. This fiber was used to strengthen polyethylene (PE) composites. Modified and unmodified cellulose fiber was characterized with inverse gas chromatography. In previous work, characterization was also carried with X-ray photoelectron spectroscopy (XPS), solid-state NMR, differential scanning calorimetry and thermogravimetry. Individual fibers were found to be covered with the corresponding esters (cellulose undecylenate, undecanoate, oleate, stearate) with partial degrees of substitution of the cellulose. Comparison of XPS and NMR results showed that the surface degree of substitution of the cellulose fiber was higher than for the bulk, showing that the esterification reaction was a surface phenomenon. The aim of this work was to acquire information on the surface characteristics of the fiber and to see whether it could be correlated to PE composite mechanical strength results. The conclusions are that polar probes seem to diffuse more into the fibers than the non-polar probes, as the non-polar component of the surface tension of the modified fiber is much lowered towards that of PE, while donor–acceptor characteristics are hardly changed by esterification. The ester with the lowest non-polar component of the surface energy, the oleate, also gives the composite with the best mechanical properties.

Keywords: Inverse gas chromatography; Paper fibre

1. Introduction

This inverse gas chromatography (IGC) study was conducted in parallel with other work on the characterisation of paper fiber esterified in heterogeneous media [1–4]. Fiber covered with esters (cellulose undecylenate, undecanoate, oleate, stearate) with partial degrees of substitution was obtained. Comparison of gravimetric, X-ray photoelectron spectroscopy (XPS) and solid state NMR showed that there was indeed an esterification gradient into the surface of the fiber. Such modified fiber, while retaining most of its crystallinity and strength, showed lower thermal stability than unmodified paper fiber [1].

1.1. IGC

In regular or classic gas–liquid or gas–solid chromatography, one is concerned with the eluting or mobile phase, which contains the substance to be separated. It is also possible to characterize the non-mobile phase, using the mobile phase and molecular probes it carries: thus the name inverse gas chromatography or IGC. Variation in surface chemistry of the non-mobile phase will change the

*Corresponding author. Tel.: +1-418-656-2437; fax: +1-418-656-5262.
E-mail address: bernard.riedl@sbf.ulaval.ca (B. Riedl).

0021-9673/02/$ – see front matter
PII: S0021-9673(02)00892-0

elution characteristics of the probes. IGC can be used to measure dispersive and acceptor–donor interactions on surfaces, with subsequent correlation with adhesion between surfaces, as obtained through mechanical properties of composites. It is particularly suited to fibrous or powdery substrates, which may be difficult to characterize by other surface characterization techniques such as contact angle measurements, because of both a rough surface and wicking phenomena. Temperature is a variable easy to vary in IGC and thus enthalpies of adsorption and related parameters are not difficult to obtain.

There are several good reviews on IGC of polymer blends or fiber/powder [5–10]. There are several instances in the literature of IGC studies on paper fiber, especially as relating to the dispersive components of the surface energy [9,10]. Lundqvist et al. [11] showed that the surface properties of various bleached pulp fibers could be broken down in dispersive and donor–acceptor contributions. The dispersive component was found to be ~45–48 mJ/m^2 and the paper had a predominantly acid surface. Birch wood meal has a mainly acid (acceptor) surface but does have basic sites.

1.2. Fiber esterification/modification

The aim of esterification with fatty acids is to make the surface of the fiber more polyethylene (PE)-like. Fiber then has better adhesion to PE continuous phase in composites. Several treatments can achieve the same result such as treatment with other esters, AKD, alkyl anhydrides, acyl chlorides and silanes. The heterogeneous esterification done here has the advantage of being simple, being carried out with inexpensive reagents, and does not reduce the strength of fiber [3]. Glasser et al. [12] found that acetylation of wood fiber resulted in much better adhesion in a thermoplastic cellulose ester/fiber composite. Effect of such and other hydrophobisation techniques was reviewed by Belgacem and Gandini [10] and Coupas et al. [13].

2. Theory

2.1. IGC principle and data reduction

In conventional chromatography, some property of an unknown sample in the moving phase is determined by its interaction with a stationary phase of known properties, whereas in IGC the properties of the stationary phase are investigated with their interaction with well characterized probes in the moving phase. The experiment involves sending a pulse of vaporizable molecules along the column containing the polymer to be characterized. The probe molecules undergo random diffusional motion in all directions, and upon this motion is superimposed a velocity U_f in the forward direction, maintained by a flow of inert carrier gas. Due to diffusion, each of the probe molecules has a velocity component U_p perpendicular to the flow direction. Any interaction with the polymer results in a retardation of the translational velocity of the probe molecules U_f. The strength and nature of the interaction can be calculated from the change in velocity using physicochemical relations presented in the following text.

By assuming that the retention mechanism is due only to surface adsorption, the residence time or retention time is inserted into the following equation, for calculating the net retention volume, V_N which is the volume of the carrier gas required to elute the probes from the column:

$$V_N = K_S A = Q(t_r - t_m) \quad (1)$$

where K_S is the surface partition coefficient of the given probe between the stationary and the mobile phases, A is the surface area (m^2) of the stationary phase, equal to the specific surface area multiplied by the sample mass, t_r (min) is the retention time of the injected probe through the column, t_m (min) is the zero retention time measured with a practically non-adsorbing probe such as methane, and Q (ml/min) is the corrected carrier gas flow-rate at column temperature and at 760 mmHg obtained as follows (1 mmHg = 133.322 Pa):

$$Q = Q_0 J \cdot \frac{T_c}{T_a} \cdot \left(1 - \frac{P_w}{P_a}\right) \quad (2)$$

where Q_0 (ml/min) is the measured flow-rate, T_c and T_a are the experimental and the ambient temperatures (K), respectively, P_a and P_w (mmHg) are the atmospheric and the saturated vapor pressure of water at ambient temperature, and J is the James–Martin compression correction term determined as follows:

$$J = \frac{3}{2} \cdot \frac{1 - \left(\frac{P_1}{P_a}\right)^2}{1 - \left(\frac{P_1}{P_a}\right)^3} \quad (3)$$

where P_1 is equal to P_a plus the pressure drop in the column.

The specific net retention volume V_g^0 at 0 °C and per gram of adsorbent is given by the following equation:

$$V_g^0 = \frac{273.15}{T_c} \cdot \frac{V_N}{W} \quad (4)$$

where W is the mass of the stationary phase.

The standard free energy ΔG_A^0, the enthalpy ΔH_A and the standard entropy ΔS_A^0 of adsorption are given by the following equations:

$$-\Delta G_A^0 = \mathrm{RT} \ln V_g^0 + C = \mathrm{RT} \ln\left(K_s \cdot \frac{P_{s,g}}{\Pi_s}\right) \quad (5)$$

$$-\Delta H_A = R \cdot \frac{\mathrm{d}(\ln V_g^0)}{\mathrm{d}\left(\frac{1}{T}\right)} \quad (6)$$

$$-\Delta S_A^0 = \frac{\Delta G_A^0 - \Delta H_A}{T} \quad (7)$$

where $P_{s,g}$ is the adsorbate vapor pressure in the gaseous standard state, equal to 101 kN/m^2, and Π_s is the spreading pressure of the adsorbed film to a reference gas phase state defined by the pressure $P_{s,g}$ of the solute, equal to 0.338 mN/m.

A linear variation of $-\Delta G_A^0$ (or $\mathrm{RT} \ln V_N$) as a function of the number of carbon atoms in the non-polar probes (*n*-alkanes) is a common observation. The free energy of adsorption corresponding to one methylene group, $-\Delta G_A^0(-CH_2-)$, was obtained through the injection of an homologous series of *n*-alkane probes:

$$-\Delta G_A^0(-CH_2-) = \mathrm{RT} \ln \frac{V_N(C_{n+1}H_{2n+4})}{V_N(C_nH_{n+2})} \quad (8)$$

V_N is the fundamental quantity used in all interpretation paths and is a measure of the interactions (adsorption/adsorption) between probe and column material.

If extremely low amounts of adsorbates are injected, adsorbate–adsorbate interactions can be neglected. Then, the following thermodynamic relationship can be applied to derive γ_S^D, the dispersive component of the surface energy of adsorbent, from V_N:

$$\mathrm{RT} \ln(V_N) = 2N(\gamma_S^D)^{1/2} \cdot a(\gamma_L^D)^{1/2} + C \quad (9)$$

where R is the gas constant, T is the temperature, N is Avogadro's number, a is the surface area of the probe molecule, γ_L^D is the dispersive component of the surface energy of the probe, and C is a constant. The dispersive component is also called the non-polar or Lifshitz–van der Waals or London component.

If *n*-alkanes are used as adsorbates, interactions are due to dispersive forces only, and hence $\mathrm{RT} \ln V_N$ is a linear function of the parameter $a(\gamma_L^D)^{1/2}$. Accordingly, γ_S^D of the adsorbent can be calculated from the slope of this ''reference line''.

Deviations in V_N from the reference line will appear when solvents capable of interacting specifically with the cellulose are used. In order to determine the contribution of the surface specific interactions in the total surface energy, it is necessary to inject polar probes in the column, in addition to *n*-alkanes.

The concept developed by Gutman [14], was applied to investigate the acid/base properties of stationary phases. According to this, compounds can be assigned a donor number *DN* expressing the basicity of the compound and an acceptor number *AN* expressing its acidity. If strongly acidic or basic adsorbates are used in IGC experiments, a measure of the acid/base character of the investigated surface is obtained from their retention volumes.

Acid–base interactions of adsorbate and adsorbent are quantified by the free energy of adsorption, ΔG^{sp}, corresponding to specific interactions, which is given by:

$$-\Delta G^{sp} = \mathrm{RT} \ln\left(\frac{V_N^{sp}}{V_N^{ref}}\right) \quad (10)$$

where V_N^{sp} and V_N^{ref} are the retention volumes of polar probes owing to specific interactions and retention volumes of *n*-alkanes (as the reference line) owing to dispersion forces, respectively.

Thus, the quantity ΔG^{sp} of an adsorbate is the vertical distance between the ordinate of the adsorbate and the reference line.

This approach can be extended to the calculation

of the free enthalpy of adsorption corresponding to specific interactions, ΔH^{sp}, by investigating the temperature dependence of ΔG^{sp} according to:

$$\Delta G^{sp} = \Delta H^{sp} - T\Delta S^{sp} \quad (11)$$

where ΔS^{sp} is the free entropy corresponding to specific interactions. ΔH^{sp} is determined as the slope of the plot of $\Delta G^{sp}/T$ versus $1/T$.

From the values of ΔH^{sp} and from the *AN* and *DN* values of some specific adsorbates, the acceptor and donor constants, K_A and K_D, for the adsorbent can be obtained using the expression:

$$\Delta H^{sp} = K_A \cdot DN + K_D \cdot AN \quad (12)$$

$\Delta H^{sp}/AN$ is linearly dependent on DN/AN and thus K_A is obtained from the plot as the slope, while K_D is obtained as the intercept. *AN* and *DN* numbers for probes, as determined experimentally by NMR and calorimetric measurements, respectively, were taken from the literature.

3. Experimental

3.1. IGC

Chromatographic measurements at infinite dilution were performed on a Hewlett-Packard 5700A apparatus equipped with dual hydrogen flame ionization detector maintained at 300 °C. To ensure flash vaporization, the temperature at the injection ports of the chromatograph was ~300 °C, which is 50 °C above the highest boiling point of the alkane probes. The probes used to evaluate the dispersive component of the surface energy of the stationary phases were *n*-alkanes ranging from *n*-hexane to *n*-nonane. The probes used in this work were purchased as chromatographically pure from Aldrich (Oakville, Canada) and were used without any further purification. The characteristics of probes are shown in Table 1.

The stationary phases were packed into copper tubing of 4.0-mm internal diameter and of different length depending on the stationary phase used in the experiment (Table 2). The column was degreased with acetone and dried before packing. The temperature of the column was controlled to within ±0.5 °C and monitored with an Omega digital thermometer. The temperature was maintained at a constant value using a circulating water bath from Julabo (Model UC-5b). Nitrogen was used as the carrier gas. The flow-rate, corrected for pressure drop along the column, and for temperature variation between the column and a soap bubble flow meter, was 30 ml/min. Methane was used as an inert marker for the death volume of the column. To ensure conditions near zero coverage such that only probe–adsorbent interactions were studied, very small quantities of

Table 1
Characteristics of injected probes [14]

Probe	Surface area of the adsorbate molecule, *a* (Å^2)	Dispersive component of the surface energy of the adsorbate, g_L^D (mJ/m^2)	Donor number, *DN* (kcal/mol)	Acceptor number, *AN* (kcal/mol)	Specific characteristic
C_6	51.5	18.4	–	–	Neutral
C_7	57.0	20.3	–	–	Neutral
C_8	62.8	21.3	–	–	Neutral
C_9	68.9	22.7	–	–	Neutral
Acetone	42.5	16.5	17.0	12.5	Amphoteric
CH_2Cl_2	31.5	27.6	–	20.4	Acidic
CH_3NO_2	37.8	26.2	2.7	20.5	Acidic
THF[a]	45.0	22.5	20.0	8.0	Basic

[a] THF: Tetrahydrofuran.

Table 2
Column description with carrier gas flow characteristics at 40 °C

Sample		DS_T	Length of the column, l (cm)	Mass of the stationary phase, W (g)	Carrier gas (N_2) flow at 40 °C, Q_0 (ml/min)	Correction factor for carrier gas flow at 40 °C, J	Carrier gas flow after the correction at 40 °C, Q (ml/min)
CEL	–	–	122	1.77	30.0	0.98	29.9
	A	0.47	62	0.94	31.0	0.99	31.7
CEL-UNA	B	1.11	62	0.93	30.5	1.00	31.1
	A	0.31	62	0.81	30.5	0.99	30.7
CEL-UNC	B	0.59	62	1.01	30.0	0.99	30.5
	A	0.08	62	0.88	30.2	0.99	30.9
CEL-OLA	B	0.14	62	0.87	31.1	0.99	31.9
	A	0.12	62	1.11	30.0	0.99	30.1
CEL-STA	B	0.19	62	1.19	30.0	0.99	30.1
PE	–	–	12	0.89	29.9	1.00	30.7

probe vapor were injected. Injections were made from 1-μl Hamilton syringe. A small amount, 0.1 μl, from the liquid probes was taken up in the syringe needle, and then pushed out completely from the syringe. The end of the needle was carefully observed. When the probe was nearly completely evaporated, the piston was pulled a little bit and injected into the injection port. Each injection was repeated several times, showing elution peaks to be reproducible. For the determination of ΔH_A^{sp} and, subsequently, K_A and K_D, measurements were performed at four different temperatures in the range 40–80 °C. A graphical technique [15,16] was used on asymmetrical peaks to obtain the retention time of the probes.

3.2. Fiber preparation/modification

The procedure for heterogeneous esterification of paper fiber used in this paper has been published [1–4] and followed the procedure of Shimizu and Hayashi [17]. Cellulose fibers, as bleached sulfite pulp (Pudget Ultra 60/40% Radiata Pine/Western Hemlock blend, provided by Georgia-Pacific, Bellingham, WA, USA) were esterified, with four different fatty acids, at two different degrees (low, high). Results on degree of substitution (*DS*) are given in Table 1.

In the text the following abbreviations are used: undecylenic acid (UNA), undecanoic acid (UNC), oleic acid (OLA), stearic acid (STA), cellulose (CEL), cellulose esters (CEL-EST), cellulose esters where organic acids with 11 or 18 carbon atoms were used in the esterification reaction (CEL-EST-11 or EL-EST-18, respectively), cellulose undecylenate (CEL-UNA), cellulose undecanoate (CEL-UNC), cellulose oleate (CEL-OLA), cellulose stearate (CEL-STA), 1-h esterification reaction (A), 2 h (B), as an example CEL-UNA-B is cellulose undecylenate synthesized after 2 h of reaction time.

Since cellulose, per repeat unit, has three –OH groups available for esterification, the mean (bulk) *DS* is anywhere between 0 and 3. In this case, DS_T, is the bulk, i.e. whole fiber, degree of substitution, determined by solid-state NMR, and varies between 0.08 and 1.11 (Tables 2 and 3). The variation from sample to sample, among the four kinds of esters and two degrees of treatment, is due to experimental difficulties in obtaining the same *DS* with different fatty acids. These DS_T correspond to rather high weight gains, from 20 to 106%. A surface atomic characterisation technique, photoelectron spectroscopy (XPS), gave a rather different picture. Values of *DS* determined by the surface oxygen concentration, give values of surface *DS*, $DS_{S(O)}$, much larger than those of DS_T [4], as shown in Table 3. This is

Table 3
Dispersive component of surface free energy (γ_S^D) and free energy of adsorption corresponding to one methylene group [$-\Delta G_A^O(-CH_2-)$] on the stationary phases as a function of the column temperatures and acid/base characteristics

Sample		DS_T	$DS_{S(O)}$	γ_S^D (mJ/m^2)					$d(\gamma_s^D)/dT$ (mJ m^{-1} K^{-1})		$-\Delta G_A^0(-CH_2-)$					$d[-\Delta G_A^0(-CH_2-)]/dT$		K_A	K_D
				20 °C[a]	40 °C	50 °C	60 °C	80 °C		R^2	20 °C[a]	40 °C	50 °C	60 °C	80 °C		R^2		
CEL	–	–	–	50.4	36.8	29.9	20.6	9.0	−0.70	0.991	3.3	2.6	2.4	2.0	1.3	−0.034	0.996	1.2	1.2
	A	0.47	1.1	39.0	30.7	25.1	20.4	12.5	−0.45	0.993	2.8	2.4	2.2	2.0	1.5	−0.022	1.000	0.8	1.3
CEL-UNA	B	1.11	1.2	35.3	26.8	23.1	18.5	10.3	−0.42	0.999	2.7	2.2	2.1	1.9	1.4	−0.022	0.995	0.8	1.4
	A	0.31	1.0	38.2	29.7	24.3	19.6	11.4	−0.45	0.996	2.8	2.4	2.1	1.9	1.5	−0.022	1.000	1.0	1.2
CEL-UNC	B	0.59	1.1	37.1	28.9	23.7	19.9	11.4	−0.43	0.998	2.8	2.3	2.1	1.9	1.5	−0.021	0.997	0.8	1.2
	A	0.08	0.6	36.2	27.7	24.3	19.3	11.3	−0.42	0.997	2.7	2.1	2.1	1.9	1.5	−0.021	0.993	0.8	1.1
CEL-OLA	B	0.14	0.6	32.4	24.6	20.5	16.2	8.8	−0.40	0.999	2.6	2.4	2.0	1.7	1.3	−0.022	0.998	0.8	1.1
	A	0.12	0.7	38.4	31.3	27.3	22.4	16.4	−0.37	0.988	2.8	2.4	2.3	2.0	1.8	−0.017	0.995	–	–
CEL-STA	B	0.19	0.9	37.7	30.2	26.2	22.0	15.3	−0.37	0.999	2.7	2.1	2.2	2.0	1.7	−0.018	1.000	0.9	1.4
PE	–	–	–	28.1	22.6	20.3	16.7	11.8	−0.27	0.994	2.4	2.1	1.9	1.8	1.5	−0.014	0.995	–	0.3

[a] Extrapolated value.

understandable as there is a gradient of esterification towards the centre of the fiber.

4. Results and discussion

4.1. Volumes of retention

As said before, cellulose fibers were treated with fatty acids. This is expected to enhance wetting of the eventual PE continuous phase of composites made with this fiber.

Table 3 shows different functions derived for IGC data. The variable is the degree of substitution of the cellulose/paper fiber. DS_T is the bulk degree of substitution, while $DS_{S(O)}$ is the surface degree of substitution derived from XPS data, with A or B degree of treatment. The value of $DS_{S(O)}$ is always greater than that of DS_T. This shows that fatty acids reacted mostly with the surface, presumably amorphous, cellulose. Since IGC is a surface characterization technique, it should possibly correlate more with XPS derived values. The depth of penetration of X-rays in XPS is quite small, in the low nm range. It is difficult to ascertain to what extent the IGC probes diffuse into the fiber surface, especially in a partly crystalline surface.

Fig. 1 is a plot of (RT $\ln V_N$) versus $a(\gamma_L^D)^{1/2}$ of the *n*-alkanes and the polar probes at different temperatures for cellulose oleate (CEL-OLA-A) and is illustrative of the kind of behaviour of these probes with all substrates here, except for PE where the values of (RT $\ln V_N$) for the polar probes lie on the alkanes curve.

Fig. 2 is a plot of $\ln V_g^0$ versus $1000/T$ for C_8 alkane on CEL, polyethylene (PE), and CEL-OLA. All such curves are linear. Curves for PE and the oleate modified fibers are quite close and distinct from the unmodified paper fiber (cellulose) curves, showing that these modified fibers are quite PE-like. Other modified fibers show the same kind of grouping around PE curves as for other non-polar probes.

Fig. 3 is a plot of $\ln V_g^0$ versus number of carbon atoms (*n*) of the *n*-alkanes at 40 °C on CEL, PE, and CEL-OLA. The same PE-like behaviour is present for all the esterified fibers.

4.2. Heats and free energies of adsorption

Fig. 4 is plot of $-\Delta H_A^0$ versus $a(\gamma_L^D)^{1/2}$ of the *n*-alkanes and the polar probes on cellulose oleate (CEL-OLA-B). All fibers show such figures, except for PE whose heats of adsorption for polar probes also fall on the alkane reference line, since PE has little or no polar sites. From the differences in values from the heats of adsorption of the polar probes from the reference line of the alkanes can be ascertained the value of the specific heats of adsorption, and from those, the values of the acid–base, or acceptor–donor, values of the fiber, as in Eq. (12).

Values of $-\Delta G_A^0(-CH_2-)$ do not vary much as a

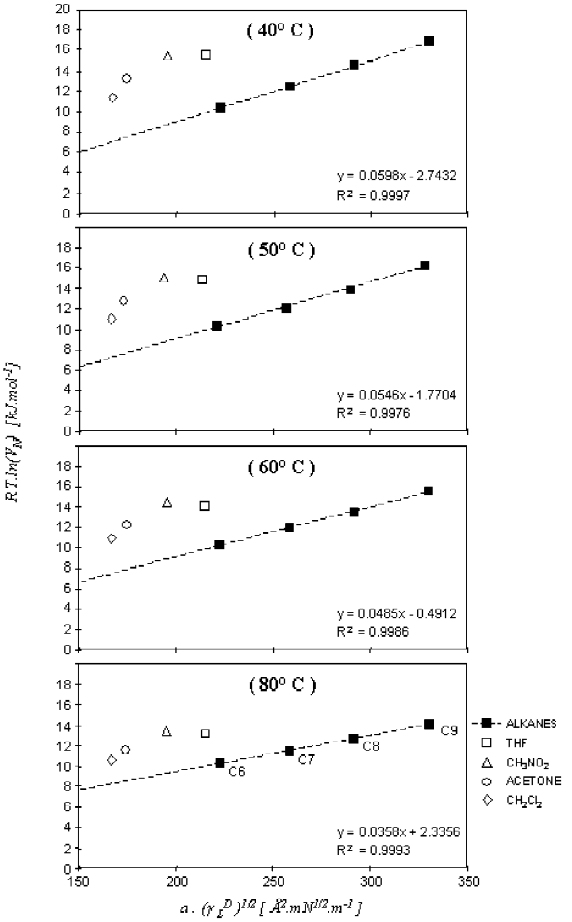

Fig. 1. Plot of RT ln V_N versus $a(\gamma_L^D)^{1/2}$ of the *n*-alkanes and the polar probes at different temperatures for cellulose oleate (CEL-OLA-A).

function of temperature or treatment, as shown in Table 3.

4.3. The dispersive component of the surface energy

Surface energy for organic material is often separated into dispersive and polar components. These are obtained with IGC or wetting techniques with non-polar and polar solvents, respectively. Generally, treatment with agents with the aim of increasing compatibility with non-polar matrices, like PE or polypropylene (PP), involve covering the surface, as is done here, with non-polar moieties, resulting in a much lowered polar component, and an, also lowered, dispersive component, albeit less so. In this case we have grafted C_{11} and C_{18} fatty acids on the surface of our paper fibers. According to the work of Kessaissia et al. [18], on silica surfaces, at constant densities of grafting, there is a gradual evolution of the surface energy as *n*, the number of carbon atoms on the fatty chain, increases. At $n=10$, the polar

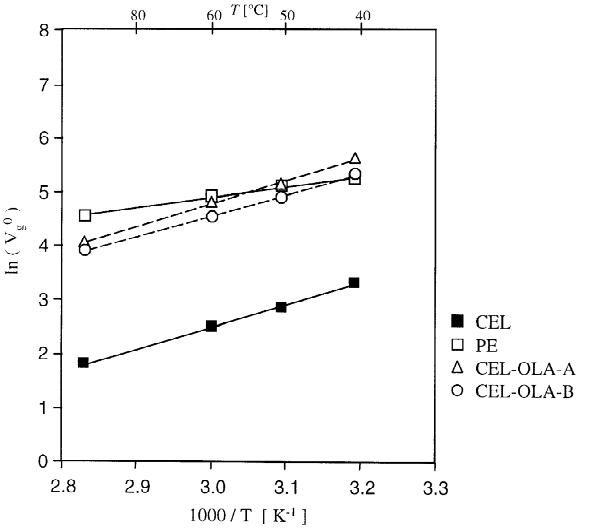

Fig. 2. Plot of $\ln V_g^0$ versus $1000/T$ for C_8 alkane on cellulose (CEL), polyethylene (PE), and cellulose oleate (CEL-OLA).

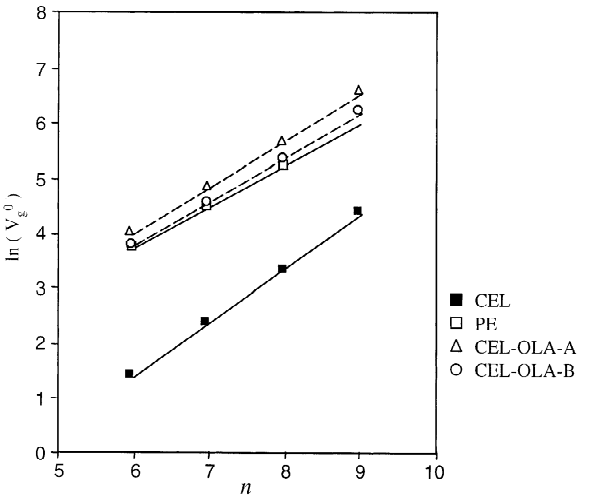

Fig. 3. Plot of $\ln V_g^0$ versus number of carbon atoms (*n*) of the *n*-alkanes at 40 °C on cellulose (CEL), polyethylene (PE), and cellulose oleate (CEL-OLA).

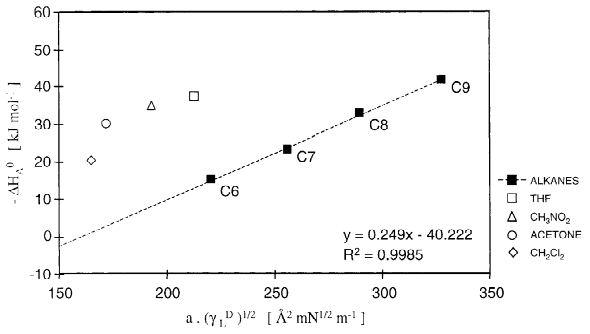

Fig. 4. Plot of $-\Delta H_A^0$ versus $a(\gamma_L^D)^{1/2}$ of the *n*-alkanes and the polar probes on cellulose oleate (CEL-OLA-B).

component of the surface energy, γ_S^P, is expected to be zero, and γ_S^D is the total surface energy. It was found also that as "*n*" increases, γ_S^D decreases from the surface energy of cellulose to γ_S^D of polyethylene at $n=16$.

Dispersive components of the surface tension, γ_S^D and as donor–acceptor (from Eq. (12)) properties were obtained (Table 3). Values of γ_S^D can be obtained from the slope of (RT $\ln V_N$) versus $a(\gamma_l^D)^{1/2}$ as in Eq. (9), from plots such as in Fig. 1. The value of γ_S^D for cellulose (bleached sulfite pulp in this case) (Table 3), at 20 °C is 50.4 mJ/m^2, very close to values of Lee and Luner [19], 48 mJ/m^2, for chromatographic paper at 25 °C, and those of Felix and Gatenholm [20] of 44.0 mJ/m^2 at 40 °C for bleached sulfite pulp (our value: 36.8 mJ/m^2). The dispersive component of unmodified fiber is rather sensitive to temperature with $d\gamma_S^D/dT$ of -0.70 mJ/m^{-2} °C^{-1}, which is a bit larger than the usual range for lignocellulosic material (-0.50 to -0.07 mJ/m^{-2} °C^{-1}) [10,21].

In general, γ_S^D decreased with esterification, and was intermediate between those of cellulose and PE. At 20 °C, the highest value of γ_S^D was 50 mJ/m^2 for cellulose/paper fiber, while the lowest was 28.1 50 mJ/m^2 for PE. For the modified celluloses/paper fiber, fiber substituted with surface *DS* of 1.1 with undecanoic acid gave the highest value of γ_S^D, 39.0 mJ/m^2 and fiber substituted with surface *DS* of 0.6 with oleic acid gave the lowest value of γ_S^D, 39.0 mJ/m^2. Also, the values of γ_S^D for more highly treated samples (A vs. B) are always lower, that is, nearer the values of PE, as expected. The temperature dependence of polar component of the surface energy, $d\gamma_S^D/dT$, for modified cellulose, is about half that of cellulose, while that of PE is a bit more than a third. Values of γ_S^D at high temperature of modified fiber were much nearer to those of PE than of unmodified fiber. In other words, as temperature increases, the modified fiber becomes more PE-like. That is a good thing since in composite manufacture, fiber and PE are melt blended near 200 °C.

It is not possible to see a variation of γ_S^D between samples grafted with C_{11} fatty acids (UNA and UNC) and C_{18} fatty acids (OLA and STA). However, there is a difference with chain length. With a DS_S near 1.1, C_{11} fatty acids, give a mean value of γ_S^D near 37.4 mJ/m^2 at 20 °C, while the C_{18} fatty acids, with a mean DS_S of 0.7, give a mean value of γ_S^D of 36.2 mJ/m^2. Thus with a lower DS_S, the C_{18} fatty acids still give a γ_S^D closer to that of PE than the C_{11} fatty acids. But it is still not that of PE, possibly because the surface is not entirely covered. However it is sufficient to lower γ_S^D by 80% of the interval between paper fiber and PE, for the oleate ester. Papirer et al. [22] did a study on stearic covered calcium carbonate: for 100% coverage, the value of γ_S^D was 27 mJ/m^2 at 20 °C (extrapolated from values at 90 °C). Thus it is probable the surface of fiber was not entirely covered with acids since our lowest value is 32.4 mJ/m^2 with the oleate.

As said before, values of γ_S^D are highly temperature dependent. At 80 °C values range from 9 to 16 mJ/m^2. These are not particularly different from values at 80 °C of γ_S^D for newsprint fiber treated with phthalic anhydride (3.9 mJ/m^2) or maleated polypropylene (5.8 mJ/m^2) [23].

4.4. Comparison with XPS results

Values of O/C vary from 0.61 for our bleached sulfite paper fiber to 0.25–0.19 for C_{11} esters and 0.28–0.17 for C_{18} esters [4]. If the surface was pure esters we would obtain ~0.17 and 0.11 for pure C_{11} and C_{18} esters, respectively. Thus the surface is not completely covered by the esters, or the X-rays penetrate beyond the ester layer to the cellulose underneath. Still those values of O/C are much nearer to those of the esters than paper fiber, confirming the highly non-polar character of the fiber surface modified by cellulose esters.

4.5. Acid–base properties

The acid–base characteristics of the fibers can be found in Table 3. Acid–base characteristics of untreated fiber are rather amphoteric, but dominant in acid component [23] with K_A of 0.65 and K_D of 0.16 for untreated newsprint fiber. Acceptor–donor, and acid–base properties (especially acid), decreased with esterification, and were intermediate between those of untreated fiber and PE (they were nearly nil for PE), but nearer to those of untreated fiber, as the *DS* was usually near 1. In Fig. 5 is a representative plot of of $-\Delta H_A^{SP}/AN$ versus DN/AN of the polar probes on CEL, PE and CEL-EST-18. All acid constants were down ~30%, which makes sense, but the donor constants for the fiber remained more or less constant. Thus although the fiber surface is partly esterified and has PE-like character, the polar probes are still able to diffuse to the underlying cellulose layers. The same phenomenon was seen by Matuana et al. [23], that is, after treatment by hydrophobic agents, γ_S^D was lowered considerably, but acid–base values were mostly unaffected. Overall, acid character of the fiber is decreased, while basic character remains stable, or is slightly enhanced, possibly due to the donor nature of ester oxygens [21].

4.6. Correlation with mechanical properties

Composites were prepared by compounding linear low-density polyethylene (LLDPE) with the same unmodified bleached sulfite fiber and esterified fiber as reinforcing filler [3]. Best results were obtained with C_{18} unsaturated esterified fiber, e.g. (CEL-OLA-B), with all other esterified fiber rather less performant. Interestingly, composites made with the oleic acid treatment, which have the lowest values of γ_S^D, that is, nearest to that of PE, gave the best composite, as ascertained by energy at yield and stress at yield. The mean value for stress at yield at 10% fiber content PE was ~14 MPa for most PE-esterified fiber, and increased to 20 MPa for CEL-OLA-B treated fiber. Energy at yield was also nearly doubled.

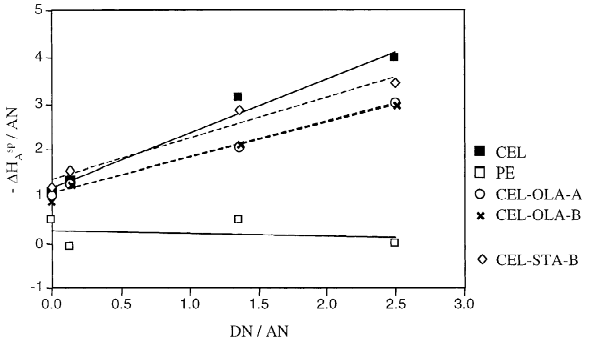

Fig. 5. Plot of $-\Delta H_A^{sp}/AN$ versus DN/AN of the polar probes on cellulose (CEL), polyethylene (PE) and CEL-EST-18.

The same series of composites were produced with addition of a crosslinking agent [3]. The use of the unsaturated esterified fiber in composites containing dicumyl peroxide, a crosslinking agent, was more effective in increasing stress at yield and energy at yield with higher cellulose esters content and degree of substitution in comparison with composites containing only cellulose fibers. The tensile properties decreased sharply in composites containing saturated cellulose esters, when used in combination with crosslinking agent, since these are unable to crosslink. Thus in this case, chemical covalent linking prevailed, even with fiber having lower γ_S^D.

4.7. Depth of interaction/esterification

Normal thickness of cell wall in wood fiber is ~8 μm. In the case of the oleate esters, the weight gain was ~25% (w/w). Since the fiber is hollow, that is, the esterification can proceed from the outer as well as from the inner surface of the fiber, and since, because of high crystallinity, the esterification is limited to the surface layer, the depth of esterification would be ~1 μm. Again, since only minor changes were found in crystallinity of the fiber [2] and fibers retained their moduli, this suggests esterification did not proceed throughout the fiber. This 1-μm depth is sufficient to lower γ_S^D by 80% of the interval between cellulose and PE.

This depth is not much different to depth of polymer coating needed to change completely from γ_S^D of wood/cellulose fiber to that of coating polymer. Simonsen et al. [24] found ~0.12–0.25 μm, and calculations from the work of Riedl and Kamdem [25] suggest ~0.5 μm at most. This again points

to the paper fiber being nearly covered with esterified cellulose.

5. Conclusion

IGC gave pertinent information on esterified cellulose fiber. The wood-cellulose oleate ester fiber, with the lowest non-polar component of the surface energy gave the best fiber PE composite. There is some difference between non-polar and polar probe variation as a function of surface modification and this may be due to different diffusion into the bulk of the probes. Also it may mean that acid–base interactions are longer range and not screened by the presence of a layer of esterified cellulose. However the 1-μm depth calculated is rather large compared to the range of acid–base interactions, so a better hypothesis is that acid–base interactions are still present within the esterified layer. Thus possibly better results would be obtained by making the continuous PE phase more polar to encourage strong acid–base interactions than to make the fiber simply more non-polar.

6. Nomenclature

Symbols

A	surface area of the stationary phase
γ_L^D	dispersive component of the surface energy of probe
γ_S^D	dispersive component of the surface energy of absorbent
ΔG_A^0	standard free energy of adsorption
$\Delta G_A^0(-CH_2-)$	free energy of adsorption of one methylene group
ΔG^{sp}	free energy of adsorption corresponding to specific interactions
ΔH_A	enthalpy of adsorption
ΔH^{sp}	enthalpy of adsorption corresponding to specific interactions
J	James–Martin compression correction term
K_A	acceptor constant
K_D	donor constant
K_S	surface partition coefficient
N	Avogadro's number
Π_s	spreading pressure
P_1	column inlet pressure
P_a	atmospheric pressure
$P_{s,g}$	absorbate vapor pressure in the gaseous standard state
P_w	saturated vapor pressure of water at ambient temperature
R	gas constant
Q	corrected carrier gas flow-rate
Q_0	measured flow-rate
ΔS_A^0	standard entropy of adsorption
ΔS^{sp}	entropy of adsorption corresponding to specific interactions
t_m	zero retention time (methane)
t_r	retention time
T_a	ambient temperature
T_c	experimental (column) temperature
V_g^0	specific net retention volume
V_N	net retention volume
$V_N(C_nH_{n+2})$	retention volume of a C_n alkane
$V_N(C_{n+1}H_{2n+4})$	retention volume of a C_{n+1}alkane
V_{ref}^N	retention volume of a non-polar probe
V_{sp}^N	retention volume of polar probe
W	mass of the stationary phase

Abbreviations

AN	acceptor number
CEL	cellulose
CEL-EST-11	cellulose esterified with a C_{11} fatty acid
CEL-EST-18	cellulose esterified with a C_{18} fatty acid
CEL-OLA	cellulose oleate
CEL-OLA-A	cellulose oleate, 1-h esterification
CEL-OLA-B	cellulose oleate, 2-h esterification
CEL-STA	cellulose stearate
CEL-STA-A	cellulose stearate, 1-h esterification
CEL-STA-B	cellulose stearate, 2-h esterification
CEL-UNA	cellulose undecylenate
CEL-UNA-A	cellulose undecylenate, 1-h esterification

CEL-UNA-B	cellulose undecylenate, 2-h esterification
CEL-UNC	cellulose undecanoate
CEL-UNC-A	cellulose undecanoate, 1-h esterification
CEL-UNC-B	cellulose undecanoate, 2-h esterification
DN	donor number
DS	degree of substitution
$DS_{s(o)}$	surface degree of substitution
DS_T	bulk degree of substitution
IGC	inverse gas chromatography
NMR	nuclear magnetic resonance
OC	oxygen/carbon atomic ratio
OLA	oleic acid
STA	stearic acid
UNA	undecylic acid
UNC	undecanoic acid
XPS	photoelectron spectroscopy or ESCA

Acknowledgements

We thank the Conseil de Recherches en Sciences et en Génie du Canada, CRSNG, the Fonds FCAR of Québec, and U. Laval for funding this work.

References

[1] P. Jandura, B. Riedl, B.V. Kokta, J. Polym. Degrad. Stab. 70 (2000) 387.
[2] P. Jandura, B. Riedl, B.V. Kokta, J. Appl. Polym. Sci. 78 (2000) 1354.
[3] P. Jandura, B. Riedl, B.V. Kokta, J. Rein. Plas. Compos. 20 (2001) 697.
[4] P. Jandura, B.V. Kokta, B. Riedl, Carbohydr. J. (2002) (in press).
[5] J.E. Guillet, in: J.H. Purnell (Ed.), New Developments in Gas Chromatography, Wiley, New York, 1973, p. 187.
[6] D.R. Lloyd, T.C. Ward, H.P. Schreiber, C.C. Pizaña (Eds.), Inverse Gas Chromatography Characterization of Polymers and Other Materials, ACS Symposium Series, Vol. 391, American Chemical Society, Washington, DC, 1989.
[7] D.J. Gray, in: A.D. Jenkins (Ed.), Progress in Polymer Science, Vol. 5, Pergamon, Oxford, 1977, p. 1.
[8] J.M. Braun, J.E. Guillet, Adv. Polym. Sci. 21 (1976) 108.
[9] B. Riedl, L. Matuana, in: A. Hubbard (Ed.), Encyclopedia of Surface and Colloid Science, Marcel Dekker, New York, USA, April, 2002, pp. 2442–2455.
[10] M.N. Belgacem, A. Gandini, in: E. Pefferkorn (Ed.), Interfacial Phenomena in Chromatography, Marcel Dekker, New York, 1999, p. 41, Ch. 2.
[11] Å. Lundqvist, L. Ödberg, J.C. Berg, Tappi J. 78 (1995) 139.
[12] W.G. Glasser, R. Taib, R.K. Jain, R.J. Kander, J. Appl. Polym. Sci. 73 (1998) 1329.
[13] A.-C. Coupas, H. Gauthier, R. Gauthier, Polym. Comp. 19 (1998) 287.
[14] V. Gutman, The Donor–Acceptor Approach To Molecular Interactions, Plenum, New York, 1978.
[15] J.R. Conder, C.L. Young, Physicochemical Measurements by Gas Chromatography, Wiley-Interscience, New York, 1979.
[16] D.P. Kamdem, B. Riedl, J. Colloid Interf. Sci. 150 (1992) 507.
[17] Y. Shimizu, J. Hayashi, Sen-I Gakkaishi 44 (1998) 451.
[18] Z. Kessaissia, E. Papirer, J.-B. Donnet, J. Colloid Interf. Sci. 82 (1981) 526.
[19] H.K. Lee, P. Luner, Nordic Pulp Paper Res. J. 2 (1989) 164.
[20] J.M. Felix, J. Gatenholm, Nordic Pulp Paper Res. J. 8 (1993) 200.
[21] A.-C. Coupas, H. Gauthier, R. Gauthier, Polym. Comp. 19 (1998) 280.
[22] E. Papirer, J. Schultz, C. Turchi, Eur. Polym. J. 20 (1984) 1155.
[23] L.M. Matuana, J.J. Balatinecz, C.B. Park, R.T. Woodhams, Wood Fiber Sci. 31 (1999) 116.
[24] J. Simonsen, Z. Hong, T.G. Rials, Wood Fiber Sci. 29 (1997) 75.
[25] B. Riedl, P.D. Kamdem, J. Adhes. Sci. Technol. 6 (1992) 1053.